



# Seasonal variations of ultra-fine and submicron aerosols in Taipei, Taiwan: implications for particle formation processes in a subtropical urban area

H. C. Cheung<sup>1</sup>, C. C.-K. Chou<sup>1</sup>, M.-J. Chen<sup>1</sup>, W.-R. Huang<sup>1</sup>, S.-H. Huang<sup>1</sup>, C.-Y. Tsai<sup>1</sup>, and C. S. L. Lee<sup>2</sup>

<sup>1</sup>Research Center for Environmental Changes, Academia Sinica, Taipei 11529, Taiwan

<sup>2</sup>Institute of Occupational Medicine and Industrial Hygiene, College of Public Health, National Taiwan University, Taipei, Taiwan

Correspondence to: C. C.-K. Chou (ckchou@rcec.sinica.edu.tw)

Received: 24 June 2015 – Published in Atmos. Chem. Phys. Discuss.: 12 August 2015

Revised: 18 December 2015 – Accepted: 4 January 2016 – Published: 5 February 2016

**Abstract.** The aim of this study is to investigate the seasonal variations in the physicochemical properties of atmospheric ultra-fine particles (UFPs,  $d \leq 100$  nm) and submicron particles ( $\text{PM}_{10}$ ,  $d \leq 10 \mu\text{m}$ ) in an east Asian urban area, which are hypothesized to be affected by the interchange of summer and winter monsoons. An observation experiment was conducted at TARO (Taipei Aerosol and Radiation Observatory), an urban aerosol station in Taipei, Taiwan, from October 2012 to August 2013. The measurements included the mass concentration and chemical composition of UFPs and  $\text{PM}_{10}$ , as well as the particle number concentration (PNC) and the particle number size distribution (PSD) with size range of 4–736 nm. The results indicated that the mass concentration of  $\text{PM}_{10}$  was elevated during cold seasons with a peak level of  $18.5 \mu\text{g m}^{-3}$  in spring, whereas the highest concentration of UFPs was measured in summertime with a mean of  $1.64 \mu\text{g m}^{-3}$ . Moreover, chemical analysis revealed that the UFPs and  $\text{PM}_{10}$  were characterized by distinct composition; UFPs were composed mostly of organics, whereas ammonium and sulfate were the major constituents of  $\text{PM}_{10}$ . The seasonal median of total PNCs ranged from  $13.9 \times 10^3 \text{ cm}^{-3}$  in autumn to  $19.4 \times 10^3 \text{ cm}^{-3}$  in spring. Median concentrations for respective size distribution modes peaked in different seasons. The nucleation-mode PNC ( $N_{4-25}$ ) peaked at  $11.6 \times 10^3 \text{ cm}^{-3}$  in winter, whereas the Aitken-mode ( $N_{25-100}$ ) and accumulation-mode ( $N_{100-736}$ ) PNC exhibited summer maxima at  $6.0 \times 10^3$  and  $3.1 \times 10^3 \text{ cm}^{-3}$ , respectively. The change in PSD during summertime was attributed to the enhancement in the pho-

tochemical production of condensable organic matter that, in turn, contributed to the growth of aerosol particles in the atmosphere. In addition, clear photochemical production of particles was observed, mostly in the summer season, which was characterized by average particle growth and formation rates of  $4.0 \pm 1.1 \text{ nm h}^{-1}$  and  $1.4 \pm 0.8 \text{ cm}^{-3} \text{ s}^{-1}$ , respectively. The prevalence of new particle formation (NPF) in summer was suggested as a result of seasonally enhanced photochemical oxidation of  $\text{SO}_2$  that contributed to the production of  $\text{H}_2\text{SO}_4$ , and a low level of  $\text{PM}_{10}$  ( $d \leq 10 \mu\text{m}$ ) that served as the condensation sink. Regarding the sources of aerosol particles, correlation analysis of the PNCs against  $\text{NO}_x$  revealed that the local vehicular exhaust was the dominant contributor of the UFPs throughout the year. Conversely, the Asian pollution outbreaks had significant influence in the PNC of accumulation-mode particles during the seasons of winter monsoons. The results of this study implied the significance of secondary organic aerosols in the seasonal variations of UFPs and the influences of continental pollution outbreaks in the downwind areas of Asian outflows.

## 1 Introduction

Due to the significant impact of particulate matter on human health and climate change, it is vital to understand the formation process of atmospheric particles (Charlson et al., 1992; Donaldson et al., 1998). A number of mechanisms have been proposed by which atmospheric particles are formed, includ-

ing binary nucleation, ternary nucleation and ion-induced nucleation for charged particles, under different environmental conditions (Kulmala, 2003; Kulmala et al., 2004, 2012). Numerous studies have been conducted in different locations to elucidate particle formation processes under various environmental settings in the free troposphere, boreal forest and coastal areas, where new particles formation processes are observed frequently (Kulmala et al., 2004, Holmes, 2007). Recently, investigations were also carried out on new particle formation within the urban boundary layer (e.g., Cheung et al., 2013, and references therein), where particle formation was suggested to be mainly influenced by the photo-oxidation of SO<sub>2</sub>. Furthermore, formation of particulate matter by heterogeneous reactions of gases on dust particles was reported recently (Hsu et al., 2014; Nie et al., 2014). Previous investigations have indicated that the air pollutants, in both gaseous and particulate form, associated with the continental outflows of air masses, could have affected a wide region in east Asia and caused severe regional air pollution (e.g., Lin et al., 2004; Wang et al., 2003; Buzorius et al., 2004). However, the formation processes of ultra-fine particles (UFPs,  $d \leq 100$  nm) and submicron particles (PM<sub>1</sub>,  $d \leq 1$  μm) under the influences of continental outflows are not yet well understood.

In urban environments, major contributing sources of aerosol particles include vehicular exhausts (e.g., Pey et al., 2008; Pérez et al., 2010), industrial emissions (Gao et al., 2009) and new particle formation by photochemical reactions (e.g., Pey et al., 2009). Approximately 55–69 % of the total particle number concentrations (PNCs) were attributed to secondary aerosols during midday in several European cities (Reche et al., 2011). In Taipei, Taiwan, a subtropical urban area, Cheung et al. (2013) observed that there was a tenfold increase in nucleation-mode particle number concentration ( $N_{9-25}$ , with size  $9 < d < 25$  nm) during new particle formation events compared to that contributed by the vehicle emission. Besides the local sources, air quality of east Asian countries is also strongly affected by the transport of air pollutants from mainland China during periods of winter monsoons (Cheung et al., 2005; Lin et al., 2004; Matsumoto et al., 2003). Lin et al. (2004) reported that the mass concentration of particulate matter (PM<sub>10</sub>) due to the long-range transport associated with winter monsoons was  $85 \mu\text{g m}^{-3}$ , about 79 % higher than that due to local pollution ( $\sim 47.4 \mu\text{g m}^{-3}$ ) in Taipei. Chemical composition of fine and coarse particles was measured during a winter monsoon period at Rishiri Island, near the northern tip of Japan, to study the transport of continental aerosols (Matsumoto et al., 2003). The results showed that higher levels of particle mass concentration were associated with the outbreaks of continental polluted air masses. In addition, Cheung et al. (2005) found deterioration in visibility around southern China during wintertime as indicated by a twofold increase in aerosol light scattering coefficient under the influences of winter monsoons. Chen et al. (2013) conducted a measurement of the particle number

concentration at the background station on the mountain of central Taiwan in summer 2009 and autumn 2010. The result showed that, on the contrary, particle number concentrations were dominated by local sources rather than long-range transport. To date, most of the relevant studies mentioned above were limited to measurements in terms of PM<sub>10</sub> or PM<sub>2.5</sub> for a particular period. The seasonal variations of particles in either ultra-fine or submicron range have not been well illustrated.

A 1-year aerosol characterization experiment was conducted in the urban area of Taipei, Taiwan. The aim of this study is to attain a better understanding of the seasonal variations of ultra-fine and submicron particles and the factors affecting particle formation, particularly under the influences of Asian monsoon circulations. In this study, we analyzed number concentration and size distribution of aerosol particles, together with the mass concentration and chemical composition of UFPs and PM<sub>1</sub> measured during four seasonal campaigns (i.e., 24 October–15 November 2012, 4–24 January, 17 March–11 April and 1–14 August 2013). The results of this study will contribute to the management strategies of the severe air pollution over the east Asia region.

## 2 Methodology

### 2.1 Observation site and instrumentation

The measurements were conducted at Taipei Aerosol and Radiation Observatory (TARO, 25.02° N, 121.53° E), located in the downtown area of Taipei, Taiwan, during October 2012 to August 2013. The measurements were carried out for 2–3 weeks in each season (see Table 1 for measurement details). The aerosol observatory is located on the top floor of Building B of the Department of Atmospheric Sciences, National Taiwan University (ASNTU), which is  $\sim 20$  m a.g.l (above ground level) (Cheung et al., 2013).

Particle number size distribution (PSD) in the range of 4–736 nm was measured by two scanning mobility particle sizer (SMPS) systems. One was equipped with a long differential mobility analyzer (long DMA, model: TSI 3081, TSI Inc.) and a condensation particle counter (CPC) (model: TSI 3022A, TSI Inc.) to measure the particles from 10 to 736 nm, which was named long SMPS. Another one was equipped with a nano-DMA (model: TSI 3085, TSI Inc.) and an ultra-fine water-based CPC (UWCPC, model: TSI 3786, TSI Inc.) to measure the particles from 4 to 110 nm, which was named nano-SMPS. The polydisperse particles were classified into selected monodisperse particles according to their electrical equivalent mobility by the DMAs. The number concentration of the monodisperse particles was then counted by the CPCs. Ambient air was drawn into the SMPS systems from outside the building through a 0.635 cm (inner diameter) conductive tube, and a sampling duration of 5 min was adopted for each PSD measurement. The SMPS systems' flow rates

**Table 1.** Median and quartile ranges (Q1–Q3) of the PNCs measured in each season. The size ranges of the PNCs are represented by the subscripted number. For example,  $N_{4-25}$  represents the number concentrations of the particles from 4 to 25 nm. The fractions of  $N_{4-25}$  and  $N_{4-100}$  of total PNCs are presented in the last two columns.

Measurement periods	$N_{4-736}$ ( $10^3$ no. $\text{cm}^{-3}$ )	$N_{4-25}$ ( $10^3$ no. $\text{cm}^{-3}$ )	$N_{25-100}$ ( $10^3$ no. $\text{cm}^{-3}$ )	$N_{4-100}$ ( $10^3$ no. $\text{cm}^{-3}$ )	$N_{100-736}$ ( $10^3$ no. $\text{cm}^{-3}$ )	$N_{4-25}/N_{4-736}$	$N_{4-100}/N_{4-736}$
Autumn 24 Oct–15 Nov 2012	13.9 (9.9–19.4)	8.6 (5.8–11.8)	3.9 (2.6–5.5)	12.7 (8.7–17.8)	1.3 (0.8–1.9)	0.62	0.90
Winter 4–24 Jan 2013	17.4 (12.7–22.3)	11.6 (8.2–15.1)	4.1 (2.8–5.6)	16.3 (11.6–21.4)	0.9 (0.5–1.5)	0.70	0.94
Spring 17 Mar–11 Apr 2013	19.4 (13.2–26.2)	10.3 (7.2–14.1)	5.8 (4.0–9.4)	17.0 (11.4–23.6)	1.9 (1.4–2.7)	0.56	0.89
Summer 1–14 Aug 2013	16.6 (9.2–26.7)	6.9 (4.5–10.4)	6.0 (2.5–11.3)	13.7 (7.9–21.4)	3.1 (0.5–5.1)	0.44	0.87

were checked weekly during the sampling period and the accuracy of the particle sizing of the DMAs was checked using polystyrene latex (PSL) spheres before the campaigns. Operation details are referred to Cheung et al. (2013).

Size-segregated aerosol samples were collected by a pair of Micro-Orifice Uniform Deposition Impactors (MOUDI, model: 110, MSP Corp.). Taking the advantage that the cut diameter of the ninth MOUDI impaction stage was exactly 100 nm, the tenth impaction stage (with a cut diameter of 56 nm) of each MOUDI was removed to allow the post-filter function as a collector of UFPs (Marple et al., 1991). The sampling flow rate of MOUDI sampler was  $30 \text{ L min}^{-1}$ . In addition, a pair of  $\text{PM}_{10}$  samplers, each consisting of a standard aerosol sampler (PQ-200, BGI Inc.) and a  $\text{PM}_{10}$  sharp cut cyclone, were deployed to collect  $\text{PM}_{10}$  samples with  $16.7 \text{ L min}^{-1}$  sampling flow rate. For both UFPs and  $\text{PM}_{10}$  sampling arrangements, one of the paired samplers was equipped with Teflon filters, whereas another was equipped with quartz fiber filters. The Teflon filter samples were used for gravimetric measurements. The quartz filter samples were deployed for the analysis of soluble ions ( $\text{Na}^+$ ,  $\text{NH}_4^+$ ,  $\text{K}^+$ ,  $\text{Ca}^{2+}$ ,  $\text{Mg}^{2+}$ ,  $\text{Cl}^-$ ,  $\text{NO}_2^-$ ,  $\text{NO}_3^-$ ,  $\text{SO}_4^{2-}$ ) using ion chromatograph (IC), and carbonaceous components (i.e., organic carbon, OC, and elemental carbon, EC) in the aerosols using a DRI-2001A carbonaceous aerosol analyzer with IMPROVE-A protocol (Chow et al., 2007). Details of the in-lab analysis are as described previously (Salvador and Chou, 2014). Both the  $\text{PM}_{10}$  and UFPs were collected with double-layered quartz filters (i.e., QBQ setup) and the artifacts due to adsorption of gaseous components were corrected as suggested by Subramanian et al. (2004). The sampling duration of each sample set (for both MOUDI and PQ-200 samplers) was from 14:00 to 12:00 LT (22 h), and a total of 69 and 75 sets of UFPs and  $\text{PM}_{10}$  samples were collected during the entire investigation period (sample sets collected in autumn, winter, spring and summer were 20, 15, 25, and 9 sets for UFPs, and 21, 16, 25 and 13 sets for  $\text{PM}_{10}$ , respectively).

Moreover, to assist the data interpretation, the hourly average mass concentration of  $\text{PM}_{10}$ , the mixing ratio of trace gases (i.e.,  $\text{NO}_x$ ,  $\text{SO}_2$  and  $\text{O}_3$ ) and the meteorology parameters (i.e., wind direction/speed and ultraviolet B (UVB, wavelength: 280–315 nm)) from the Guting air quality station of Taiwan Environmental Protection Agency, which is about

1 km from TARO, were analyzed in this study. The details of instrumentation setup for trace gas measurements are referred to Cheung et al. (2013).

## 2.2 Data processing and analysis

The PSD of 4–736 nm presented in this study was combined from two sets of SMPS data, where the nano-SMPS corresponded to the size range of 4–50 nm, and the long-SMPS corresponded to the size  $> 50$  nm. The diffusion loss of the particles during the sample transport in the tubing was corrected according to the algorithm proposed by Holman (1972). Particle number concentrations for different size ranges were then calculated from the SMPS measurements.

The 5 min PSD data were synchronized into hourly averages, and fitted by the DO-FIT model developed by Hussein et al. (2005) according to the multiple log-normal distribution algorithms. Based on the fitted PSD data, the PNCs were classified into  $4 \leq d \leq 25$  nm ( $N_{4-25}$ ),  $25 < d \leq 100$  nm ( $N_{25-100}$ ),  $4 \leq d \leq 100$  nm ( $N_{4-100}$ ),  $100 < d \leq 736$  nm ( $N_{100-736}$ ) and  $4 \leq d \leq 736$  nm ( $N_{4-736}$ ), for nucleation-mode, Aitken-mode, ultra-fine, accumulation-mode and total particles, respectively. The Pearson correlation coefficient,  $r$ , was calculated by PASW Statistics ver. 18 (SPSS Inc.) to determine the correlation between the respective parameters.

## 2.3 Classification of new particle formation and calculation of the particle growth and formation rates

A new particle formation (NPF) event is defined as the increase of the number concentration of nucleation-mode particles, which are growing into Aitken- and/or accumulation-mode size range ( $\geq 25$  nm) and last for a few hours until they coagulate on the pre-existing aerosol and/or other surfaces in the atmosphere. The calculation of particle growth rate was represented by the rate of geometric median diameter changes during the period of nucleation-mode particles growing through 25 nm (Cheung et al., 2013). The formation rate ( $J$ ) of nucleation-mode particles for each NPF event was calculated for the particle size ranging from 4 to 25 nm according to the method of Dal Maso et al. (2005). The formation rate is defined as the sum of the apparent formation rate

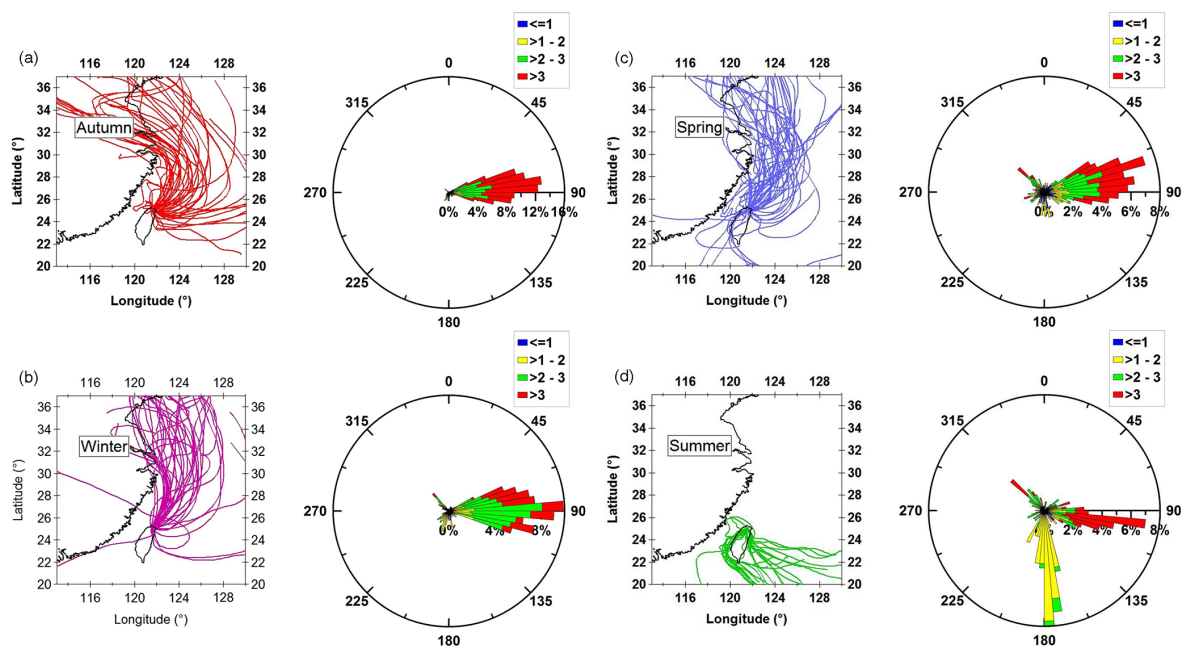


**Figure 1.** Back trajectories calculated for Taro for the measurement periods (left panel) and surface wind rose plots (right panel) in (a) autumn, (b) winter, (c) spring and (d) summer. The color codes of wind rose plots represent the wind speed: blue  $< 1 \text{ ms}^{-1}$ ; yellow  $1\text{--}2 \text{ ms}^{-1}$ ; green  $2\text{--}3 \text{ ms}^{-1}$ ; red  $> 3 \text{ ms}^{-1}$ .

( $dN_{4-25}/dt$ ) and the coagulation loss rate during the NPF event. It should be noted that the reported apparent particle formation rate is expected to be smaller than the actual nucleation rate, since some fraction of formed nuclei are always scavenged by coagulation into larger pre-existing particles before they grow larger by condensation (Lehtinen et al., 2007). The work done by Kulmala et al. (2012) is referred to for an overview of the methodology on the measurement of the nucleation of atmospheric particles.

## 2.4 Back trajectory analysis

Backward trajectories were calculated using the HYSPLIT model (Hybrid Single Particle Lagrangian Integrated Trajectory, Version 4.9) of NOAA (National Oceanic and Atmospheric Administration) (Draxler, 1999) for Taro during the sampling period, in order to trace the origins of the air masses. Seventy-two-hour back trajectories were calculated twice per day at 00:00 and 12:00 LT with a height setting of 200 m a.g.l. It should be noted that the grid resolution of the meteorological data used for the calculation of back trajectories is  $1^\circ \times 1^\circ$ , which is not enough to trace the detailed air mass passage over the scale of the study region and, therefore, the trajectories only provide an indication of the region from which the air mass was originated.

## 3 Results and discussions

### 3.1 Particle number concentration and size distribution in respective seasons

As mentioned above, the air quality of Taipei is significantly affected by both the local vehicular exhausts and long-range transport of air pollutants, of which the latter is dominated by meteorological factors. The information on the meteorological conditions, particularly the wind pattern, is important to elucidate our results and is thus presented here. The back trajectories of the air masses for Taro are illustrated in Fig. 1 (left panel). The results showed that northeasterly winds prevailed in autumn and winter seasons, passing through the Asian continent before reaching Taiwan, whereas southerly winds prevailed in summertime. The air masses observed in the spring period were found to mainly be associated with Asian continental outflows and occasionally associated with the southerly flows. This observation agreed with the surface wind direction measured in the Taipei area (see Fig. 1, right panel), where northeasterly winds dominated during the period from November 2012 to May 2013, and southerly winds prevailed from May to August 2013.

The particle number concentrations in various size ranges during each season are summarized in Table 1. Relatively higher total PNCs ( $N_{4-736}$ ) were observed in spring and winter with median values of  $19.4 \times 10^3$  and  $17.4 \times 10^3 \text{ cm}^{-3}$ , respectively, followed by that of summer ( $16.6 \times 10^3 \text{ cm}^{-3}$ ) and autumn ( $13.9 \times 10^3 \text{ cm}^{-3}$ ). This result is comparable to

the previous measurements conducted in urban Taipei where the seasonal means of PNCs ( $10 < d < 560$  nm) ranged from  $11.0 \times 10^3$  to  $17.0 \times 10^3$  cm<sup>-3</sup> (Cheng et al., 2014). Figure 2 illustrates the number, surface and volume size distributions of the aerosol particles. The geometric mean diameter (GMD) of each PSD mode was retrieved from the number concentration data. The GMDs of the nucleation, Aitken and accumulation modes were found to be 10.4–12.8, 26.5–38.4 and 91.8–159.0 nm, respectively. Details of particle number concentration and GMDs of each fitted mode in four seasons are listed in Table S1 in the Supplement.

In addition, the fitted GMDs of surface distribution were found to be 77.4 and 293 nm for autumn, 22.1, 68.9 and 228 nm for winter, 77.4 and 253 nm for spring and 12.9 and 268 nm for summer, respectively (not shown in the figures). In winter and summer seasons, one of the fitted surface GMDs was located at nucleation mode, showing the significant contribution of nucleation-mode particles in these two seasons. Bimodal volume distribution was obtained for all seasons where the fitted volume GMDs were 96.3 and 372 nm for autumn, 71.8 and 275 nm for winter, 99.5 and 339 nm for spring and 99.5 and 237 nm for summer, respectively. The GMD of first volume mode was relatively stable in each season (i.e., 71.8–99.5 nm), but a smaller GMD (237 nm) for the second volume mode was observed in summer. The results implied that a higher fraction of particles could have evolved from smaller size range (i.e., nucleation and Aitken modes) into accumulation mode, which coincided with our observation that NPF events occurred mostly in summer (see Sect. 3.4). Furthermore, this seasonal variability agrees with our previous findings that the growth rate of newly formed particles was correlated with the photolysis of ozone, an indicator of photochemical activity (Cheung et al., 2013). The causes responsible for the observed seasonal variations in PNCs will be detailed in the following sections. This was different from that observed in urban Beijing where a relatively larger GMD was observed in accumulation mode due to the enhancement of condensation by higher photochemical activities in summer, but without significant seasonal variations in Aitken-mode distribution (Wu et al., 2008).

It was revealed that the nucleation-mode particles were predominant in the PNCs during autumn, winter and spring in the study area, whereas a distinct size distribution pattern was observed in summertime. In summer, the fraction of nucleation ( $N_{4-25}/N_{4-736}$ ) decreased to 0.44 (see Table 1) and the Aitken-mode PNCs increased to be comparable to that of the nucleation mode, whereas the  $N_{4-25}/N_{4-736}$  ratios for other seasons ranged from 0.56 to 0.77 (see Table 1). An observation from another aspect is that the PNC of nucleation mode ( $N_{4-25}$ ) peaked in winter and reached the minimum in summer; whereas the PNCs of Aitken mode ( $N_{25-100}$ ) and accumulation mode ( $N_{100-736}$ ) reached their maxima in summertime. The changes in the size distribution in summer season were most likely due to the seasonally enhanced pho-

tochemical production of condensable vapors that, in turn, contributed to the growth of aerosol particles in the atmosphere.

### 3.2 Mass concentration and chemical composition

Figure 3a and b illustrate the average chemical composition and mass concentration of UFPs and PM<sub>1</sub>, respectively, for each season. Details of the mass concentration and chemical composition of UFPs and PM<sub>1</sub> are listed in Table S2 in the Supplement.

The seasonal means of UFPs ranged from 0.73 to 1.64 μg m<sup>-3</sup>, with an annual average of 1.01 μg m<sup>-3</sup>. The measured mass concentration of UFPs of the present study was comparable to that in the urban area of Los Angeles, United States (0.80–1.58 μg m<sup>-3</sup>, Hughes et al., 1998), and relatively higher than that in urban Helsinki, Finland (average 0.49 μg m<sup>-3</sup>, Pakkanen et al., 2001). For the chemical composition, OC was found to be the major mass contributor, which accounted for 29.8 % (seasonal means ranging from 26.9 to 33.4 % for various seasons) of average mass concentration of UFPs. The EC was the second major component with an average mass contribution of 5.1 % (seasonal means 2.4–7.6 %), followed by sulfate (SO<sub>4</sub><sup>2-</sup>) at 4.3 % (seasonal means 3.4–6.4 %) and nitrite (NO<sub>2</sub><sup>-</sup>) at 2.9 % (seasonal means 0.9–7.3 %). In addition, a large fraction of mass was contributed by the group of “others”, which consisted of mineral (K<sup>+</sup>, Ca<sup>2+</sup>, PO<sub>4</sub><sup>3-</sup> and Mg<sup>2+</sup>), sea salt (Na<sup>+</sup> and Cl<sup>-</sup>) and unidentified species. The results showed that, on average, mineral and sea salt components attributed only 3.5 % (seasonal means 2.0–6.0 %) to UFPs mass concentration. Thus a substantial amount of UFPs remained unidentified, which likely included hydrogen and oxygen associated with OC. The conversion factors used to estimate the average molecular weight per carbon in particulate organic matter varied depending on the characteristic of aerosols. A lower factor value, 1.2, was usually suggested for saturated organic molecules, while a higher value, 1.6, was adopted for water-soluble compounds consisting of multifunctional oxygenated groups; and even higher factor values were suggested for aged aerosols which contained a higher portion of low and semi-volatile products of photochemical reactions (Turpin and Lim et al., 2001). The high unidentified mass fraction implied that the photochemical production of secondary organic aerosols was a significant process responsible for the elevated levels of UFPs observed in this study.

As shown in Fig. 3b, average PM<sub>1</sub> was estimated to be 14.7 μg m<sup>-3</sup> (seasonal means 11.6–18.5 μg m<sup>-3</sup>) in this study, which is similar to the results of a previous study in urban Taipei (average 14.0 μg m<sup>-3</sup>, Li et al., 2010). The measured PM<sub>1</sub> level is relatively higher than that of the urban areas of Phoenix, United States (5.9 μg m<sup>-3</sup>, Lundgren et al., 1996), and Helsinki, Finland (6.1 μg m<sup>-3</sup>, Vallius et al., 2000). For chemical composition, sulfate was the major mass contributor of PM<sub>1</sub> (average 39.0 %, seasonal means

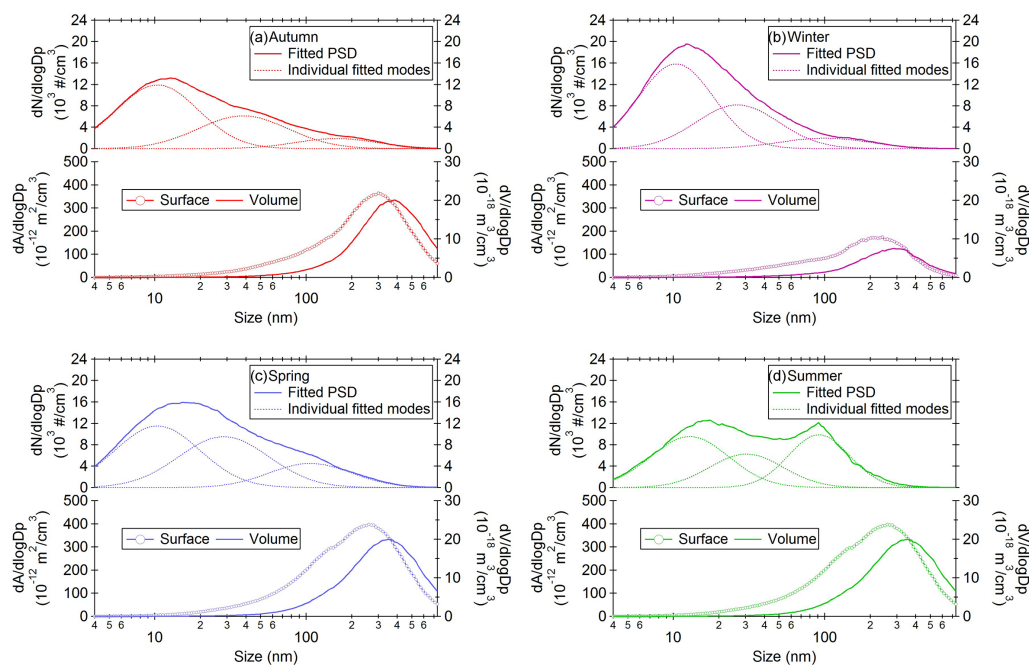


**Figure 2.** Size distribution of particle number (upper panel), and surface and volume (lower panel) concentrations measured in (a) autumn, (b) winter, (c) spring and (d) summer (by curve fitting).

33.8–46.8 %), followed by ammonium (average 12.7 %, seasonal means 12.0–13.2 %) and OC (average 11.5 %, seasonal means 9.2 to 14.3 %).

The results presented above indicated that UFPs exhibited a distinct seasonal variability and composition from  $PM_{10}$  in the study area. The highest concentration of UFPs was observed in summer ( $1.64 \mu\text{g m}^{-3}$ ) and the lowest in winter ( $0.73 \mu\text{g m}^{-3}$ ). This result may be attributed to the stronger photochemical activities in summer, which could have enhanced the formation of secondary organic aerosols. Consequently, the mass concentration of OC increased from  $0.20 \mu\text{g m}^{-3}$  in winter to  $0.47 \mu\text{g m}^{-3}$  in summertime. It is noteworthy that the mass concentration of sulfate in UFPs also peaked in summer ( $64 \text{ ng m}^{-3}$ ), suggesting enhancement in the photo-oxidation of  $\text{SO}_2$ . Cheung et al. (2013) found that photo-oxidation of  $\text{SO}_2$  was the major mechanism for the formation of new particles in Taipei, Taiwan, and the production of condensable vapors was also dominated by photo-oxidation. The covariations in sulfate and OC revealed in this study further suggested that secondary organic compounds were the major condensable matter contributing to the growth of newly formed particles.

While the organics predominated in the mass concentration of UFPs, which included nucleation-mode and Aitken-mode particles, the measurements of  $PM_{10}$  in this study suggested that sulfate was the major constituent of accumulation-mode aerosols. In contrast to the seasonal variation of UFPs, the mass concentration of  $PM_{10}$  reached a maximum at  $18.5 \mu\text{g m}^{-3}$  in spring and exhibited a mini-

mum at  $11.6 \mu\text{g m}^{-3}$  in summer. The  $PM_{10}$  differences between spring and summer were mostly due to declined ambient levels of sulfate, nitrate and ammonium ions. As a result, the mass contribution of the three inorganic ions in  $PM_{10}$  reduced from 55.7 to 46.2 % and, conversely, the mass fraction of OC increased from 10.2 to 14.3 %. The seasonal characteristics of  $PM_{10}$  concentration and composition were mostly attributed to the changes in the origin areas of background air mass, which shifted from the Asian continent to the western Pacific Ocean during summertime (see Fig. 1). Our previous studies reported that the fine particulate matter ( $PM_{2.5}$ ) transported on the Asian outflows to northern Taiwan maximized in springtime and were enriched in sulfate, nitrate and ammonium (Chou et al., 2008, 2010). The seasonal variability of  $PM_{10}$  found in this study was consistent with the previous observations for  $PM_{2.5}$  and thereby suggested the significance of Asian outflow aerosols to the  $PM_{10}$  budget in the downwind areas of the Asian continent.

### 3.3 Seasonal characteristics of photochemical production

In order to study the influences of photochemical production of particles, the measurements of PNC and PSD were analyzed per daytime (07:00–17:00 LT) and nighttime (17:00–07:00 LT), respectively (see Fig. 4). In urban environments, the possible sources influencing the PNC and PSD are complicated, which include not only the direct emission from primary sources but also the interaction between the newly

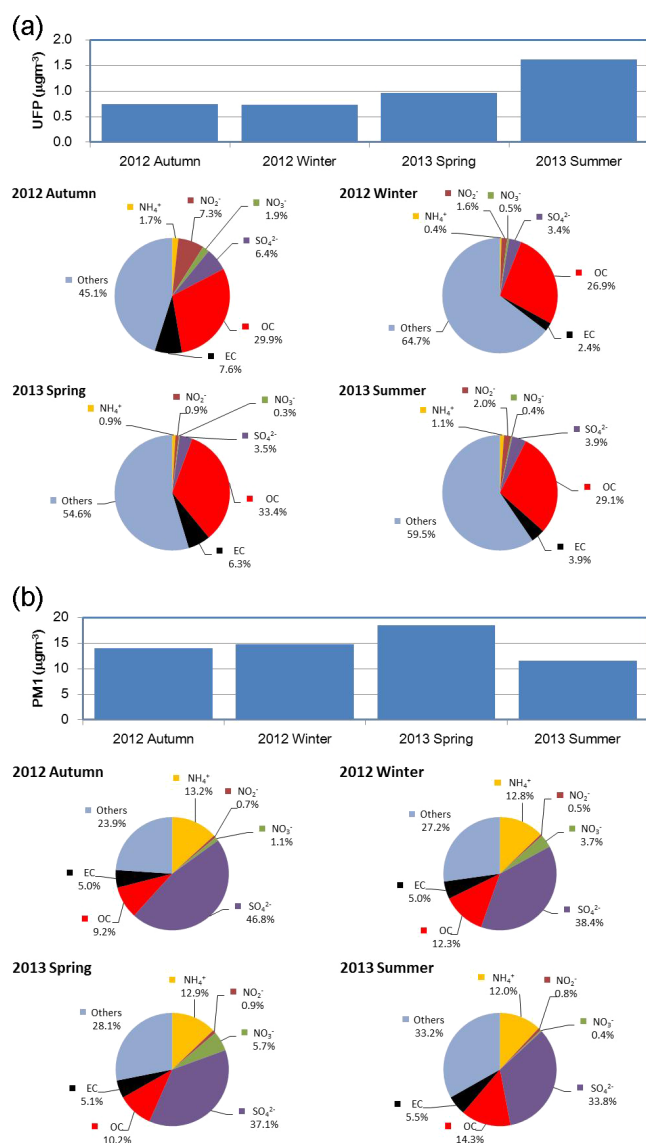


**Figure 3.** Seasonal average concentration and composition of (a) ultra-fine (UFPs) and (b) submicron (PM<sub>1</sub>) particles observed at TARO in Taipei, Taiwan, from autumn 2012 to summer 2013.

formed particles, pre-existing particles and condensing vapors through condensation and coagulation processes. Nevertheless, these processes occurred throughout the day and will not dominate in the differences between daytime and nighttime PNCs as observed in this study. It was assumed that the photochemical reaction was the major attributing factor to the observed diurnal differences in PNC. Since the particles in nighttime were mainly emitted from the vehicular exhausts and the elevated PNCs in daytime were due to both the primary and secondary sources of the particles in the study area (Cheung et al., 2013), a larger difference between the PNCs observed in daytime and nighttime indicated stronger influences of photochemical production on the PNCs. The most

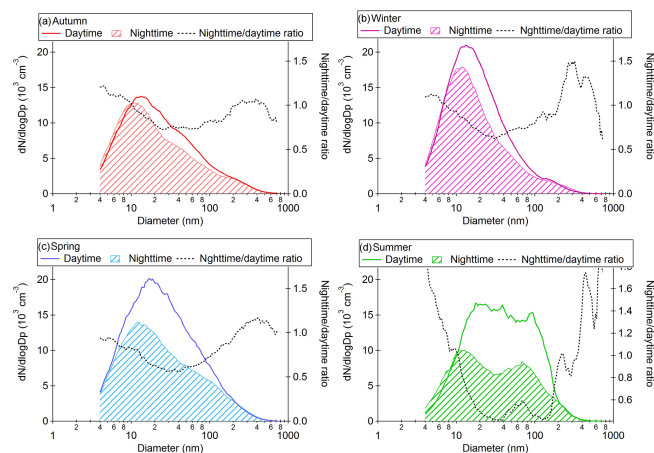


**Figure 4.** Median PSDs measured during the daytime (07:00–17:00LT) and nighttime (17:00–07:00) in (a) autumn, (b) winter, (c) spring and (d) summer.

striking seasonal feature shown in Fig. 4 is the large difference between daytime and nighttime PSD in summer as indicated by the low  $N_{4-736}$  (nighttime)/ $N_{4-736}$  (daytime) ratio; whereas higher ratios were observed in other seasons. In addition, the diurnal variation of particle size distribution (see Fig. 5) provided further information about the variations in PSD. Two nucleation bursts were distinctly observed in morning and afternoon traffic peak hours in autumn, winter and spring, while a typical PSD pattern of nucleation events (an increase of nucleation-mode particle concentrations with subsequent growth in particle size) was dominant in summer. This result is as expected because the photochemical production of nucleation-mode particles is more intense during warm seasons (Cheung et al., 2011). Moreover, as discussed in the previous section, the photochemical reactions could produce condensable organics, which allows the newly formed nucleation-mode particles to grow into the Aitken mode. The relatively small differences between the daytime and nighttime  $N_{4-736}$  in autumn and winter indicated that the photochemical contribution in PNCs had declined as compared to that in summertime. Nevertheless, the contribution of vehicle emission was also significant, especially during colder seasons and when photochemical reactions were less intense. This will be discussed in detail in Sect. 3.5.

### 3.4 Factors affecting new particle formation (NPF)

As shown in a previous study, the NPF events were frequently observed in summer, which subsequently induced a notable increase in  $N_{4-25}$  in Taipei (Cheung et al., 2013). The frequency of NPF events was found to be 10 out of 84 measurement days and the events were observed in autumn (1 out of 23 days), spring (3 out of 26 days) and summer (6 out of 14 days) seasons. Figure 6a–d show the scatter plots of  $N_{4-25}$  against  $\text{NO}_x$  for daytime in each season. During

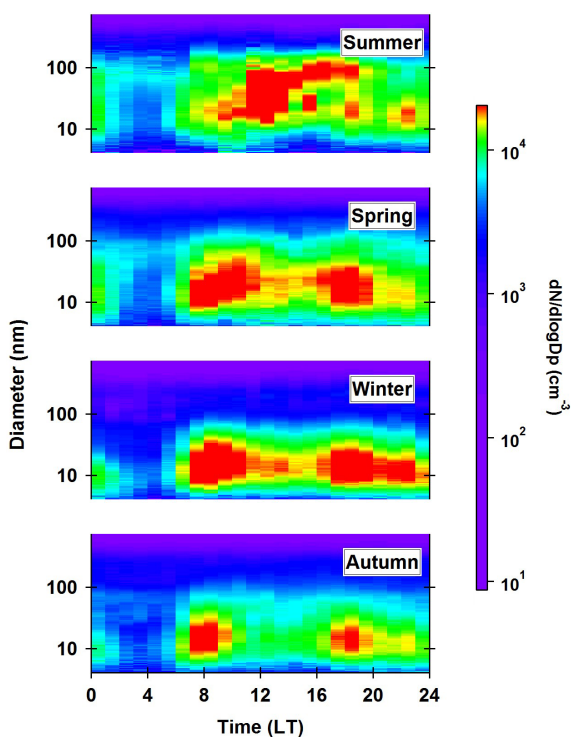


**Figure 5.** Diurnal variation of particle number size distribution in each season. From the lower panel to the top panel: autumn, winter, spring and summer.

the NPF events, a nonlinear relationship between these two parameters was usually observed during the daytime (Cheung et al., 2013). The results showed that clear NPF events were observed often in summer and occasionally in spring, but rarely in autumn and winter in the study area. The average particle growth and formation rates were found to be  $4.0 \pm 1.1 \text{ nm h}^{-1}$  and  $1.4 \pm 0.8 \text{ cm}^{-3} \text{ s}^{-1}$ , which are comparable to those measured in other urban studies in Asian cities such as Hong Kong (average  $6.7 \text{ nm h}^{-1}$ , Wang et al., 2014) and Beijing (average  $5.2 \text{ nm h}^{-1}$ , Wang et al., 2013), and also within the range observed in other nucleation studies across the globe ( $\sim 1\text{--}20 \text{ nm h}^{-1}$ , Kulmala et al., 2004). The particle growth and formation rates of each case are listed in Table 2.

Table 3 summarizes the averages of  $N_{4-25}$ ,  $\text{PM}_{10}$ , the  $\text{H}_2\text{SO}_4$  proxy (as  $\text{UVB} \cdot \text{SO}_2 / \text{condensation sink}$ ) and wind speed for each season. Petäjä et al. (2009) calculated the  $\text{H}_2\text{SO}_4$  proxy with a pre-factor value,  $k$ , and used it to estimate the actual sulfuric acid concentration. The estimation of a site-specific  $k$  value requires an actual measurement of  $\text{H}_2\text{SO}_4$ , which is not available in this study area. The proxy value calculated in this study was therefore only used as an indicator of particle production strength contributed by  $\text{H}_2\text{SO}_4$ . The dominating factors associated with the frequent particle formation in summertime were the low  $\text{PM}_{10}$  concentration ( $35.6 \mu\text{g m}^{-3}$ ) and high  $\text{H}_2\text{SO}_4$  proxy ( $493.1 \text{ ppb W m}^{-2} \text{ s}$ ). The association of sulfuric acid pro-

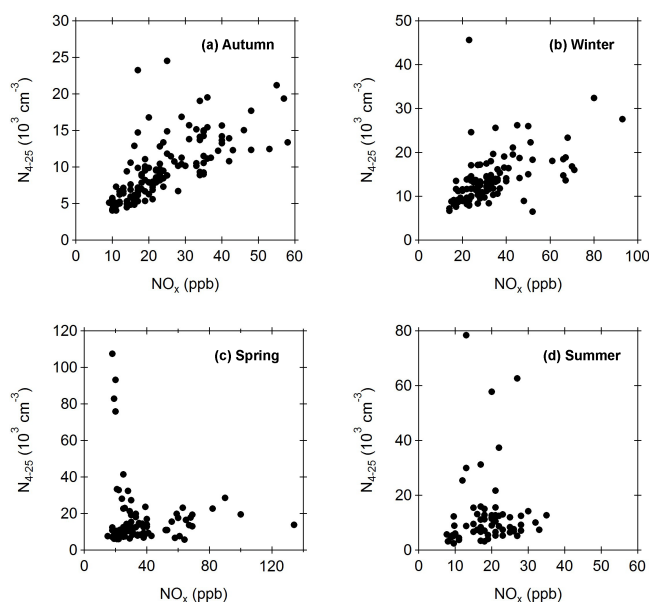


**Figure 6.** Scatter plots between hourly  $N_{4-25}$  and  $\text{NO}_x$  observed in (a) autumn, (b) winter, (c) spring and (d) summer at the TARO site during the period of 07:00–17:00 LT.

duction and the NPF events agreed with the elevated mass concentration of sulfate in UFPs during summertime (shown in Table S2), as well as the results of previous urban studies (Woo et al., 2001; Cheung et al., 2013). This strongly suggested that the new particle formation was mainly driven by the photochemical oxidation of  $\text{SO}_2$  under low condensation sink conditions (Gao et al., 2009; Nie et al., 2014), where the  $\text{SO}_2$  could be transported from the upwind area on the summer monsoons (see Fig. 1d). Contrarily, the absence of particle formation events in wintertime could be attributed to the declined photochemical production of  $\text{H}_2\text{SO}_4$  as well as the suppression of NPF by particles transported from the Asian continent (Lin et al., 2004). The results of this work evidenced that low  $\text{PM}_{10}$  concentration and high sulfuric acid production favored the particle formation process in urban areas. Nevertheless, it should be noted that condensing vapors other than sulfuric acid, for example volatile organic compounds, could also contribute to the observed particle formation, which requires further investigation.

The scatter plot between  $\text{UVB} \cdot \text{SO}_2$  and condensation sink is depicted in Fig. 7. Relatively higher  $\text{UVB} \cdot \text{SO}_2$  values were obtained during NPF events. Notably, there was a group of data with high  $\text{UVB} \cdot \text{SO}_2 / \text{CS}$  but low  $\text{UVB} \cdot \text{SO}_2$  where no NPF event was observed. This implied that there could be a threshold level of  $\text{UVB} \cdot \text{SO}_2$  for NPF in the study region. However, some exceptions existed in the data set and suggested that the parameters driving NPF have not been well accounted for and need to be studied further. It was also noticed that an Asian outflow event occurred on 7 April 2013 during which an atypical NPF was observed (labeled with a

**Table 2.** Time periods defined as the new particle formation events and the particle growth and formation rates.

Date	Time period (LT)	Growth rate (nm h <sup>-1</sup> )	Formation rate (cm <sup>-3</sup> s <sup>-1</sup> )
9 Nov 2012	07:00–13:00	3.4	1.30
26 Mar 2013	06:00–10:00	3.4	1.91
4 Apr 2013	07:00–10:00	3.7	1.13
5 Apr 2013	08:00–12:00	5.5	1.10
4 Aug 2013	09:00–12:00	3.9	1.84
5 Aug 2013	09:00–13:00	4.9	2.44
7 Aug 2013	06:00–12:00	3.5	0.84
8 Aug 2013	09:00–12:00	5.0	2.76
9 Aug 2013	06:00–13:00	1.6	0.39
11 Aug 2013	06:00–09:00	4.8	0.58
Average (± standard deviation)		4.0 (±1.1)	1.4 (±0.8)

**Table 3.** Average of N<sub>4–25</sub>, PM<sub>10</sub>, UVB, SO<sub>2</sub>, condensation sink (CS), H<sub>2</sub>SO<sub>4</sub> proxy and wind speed of different seasons. Standard deviation values are shown in parentheses. (Note: the data of the rainfall observations were not used in the calculations.)

Periods	N <sub>4–25</sub> (10 <sup>3</sup> no. cm <sup>-3</sup> )	PM <sub>10</sub> (µg m <sup>-3</sup> )	UVB (Wm <sup>-2</sup> )	SO <sub>2</sub> (ppb)	CS (10 <sup>-2</sup> s <sup>-1</sup> )	H <sub>2</sub> SO <sub>4</sub> proxy (ppb Wm <sup>-2</sup> s)	Wind speed (ms <sup>-1</sup> )
Autumn	8.6 (±4.5)	53.9 (±21.4)	1.04 (±1.75)	2.27 (±1.44)	0.8 (±0.5)	307.1 (±609.1)	2.8 (±1.0)
Winter	11.6 (±9.2)	48.4 (±23.9)	0.80 (±1.47)	2.58 (±1.61)	0.8 (±0.6)	240.0 (±472.1)	2.3 (±0.9)
Spring	10.2 (±9.2)	61.1 (±27.0)	0.99 (±1.73)	2.76 (±1.67)	1.4 (±0.7)	238.4 (±533.6)	2.2 (±1.2)
Summer	6.9 (±9.1)	35.6 (±13.7)	1.97 (±2.95)	3.19 (±2.55)	1.9 (±1.5)	493.1 (±1066)	2.3 (±1.1)

black dot in Fig. 7). This could be relevant to the secondary particle formation on dust surface under the influence of the long-range transport of air mass. This will be discussed in further detail in Sect. 3.6.

### 3.5 Influences of local emission on PNCs

Vehicle emission is known to be the major source of particulate matter in urban environment, particularly during nighttime. In order to investigate the relationship between the vehicular exhausts and PNCs, the scatter plots of NO<sub>x</sub> (as an indicator of vehicle emission) against N<sub>4–25</sub>, N<sub>25–100</sub> and N<sub>100–736</sub> during nighttime were examined for winter and summer periods (see Fig. 8). The values of the Pearson correlation coefficient (*r*) and the slope of linear regression between NO<sub>x</sub> and PNCs are summarized in Table 4.

The highest *r* values were found in both the plots of NO<sub>x</sub> against N<sub>25–100</sub> for winter (*r* = 0.88) and summer (*r* = 0.87). This result suggested a strong linear correlation between the vehicle emission and the N<sub>25–100</sub> which coincided with the results from previous studies (e.g., Morawska et al., 2008). During wintertime, stronger correlation was found between NO<sub>x</sub> and N<sub>4–25</sub> (*r* = 0.84) and N<sub>25–100</sub> (*r* = 0.88) compared to that between NO<sub>x</sub> and N<sub>100–736</sub> (*r* = 0.38). In contrast, high *r* values were obtained between NO<sub>x</sub> and all particle modes in summer (*r* = 0.70–0.87). The robust correlation of NO<sub>x</sub> and N<sub>4–25</sub>, as well as NO<sub>x</sub> and N<sub>25–100</sub>,

suggested that local vehicle emission was the predominant source of UFPs throughout a year. These results coincided with previous studies on the size distribution of vehicle exhaust particles, which were found to be 20–130 and 20–60 nm, respectively, for diesel and petrol engine vehicles (Harris and Maricq, 2001; Ristovski et al., 2006). However, the PNCs of accumulation-mode particles (N<sub>100–736</sub>) in winter were dominated by NO<sub>x</sub>-independent sources, which were most likely related to the pollution outbreaks from the Asian continent. Lin et al. (2004) indicated that the long-range transported air mass was characterized by a high level of PM<sub>10</sub> and a low mixing ratio of NO<sub>x</sub> due to its short atmospheric lifetime. Interestingly, a moderate correlation between the PNC of accumulation-mode particles (N<sub>100–736</sub>) and NO<sub>x</sub> was also observed in summer. Given that the Asian outflow ceased in summertime, this correlation evidenced a substantial contribution of local sources, particularly vehicular emissions, to the PNC of accumulation-mode particles in Taipei, Taiwan.

The slope values can serve as a relative emission factor of particles per NO<sub>x</sub>, which indicates the degree of influence of vehicle emission on the PNCs (Cheung et al., 2013). The corresponding slope values for N<sub>4–25</sub>, N<sub>25–100</sub> and N<sub>100–736</sub>, were found to be 279, 163 and 18 cm<sup>-3</sup> ppb<sup>-1</sup> in winter, and 239, 330 and 155 cm<sup>-3</sup> ppb<sup>-1</sup> in summer. A larger sum of slope values (724 vs. 460 cm<sup>-3</sup> ppb<sup>-1</sup>) was found in summertime compared to the winter period, evidencing a greater

**Table 4.** Pearson correlation coefficient ( $r$ ) and slope of linear regression of PNCs against  $\text{NO}_x$  during the nighttime (20:00–04:00 LT) in winter and summer periods.

Periods		$N_{4-25}$	$N_{25-100}$	$N_{100-736}$
Winter	Slope	279	163	18
	$r$	0.84	0.88	0.38
Summer	Slope	239	330	155
	$r$	0.76	0.87	0.70

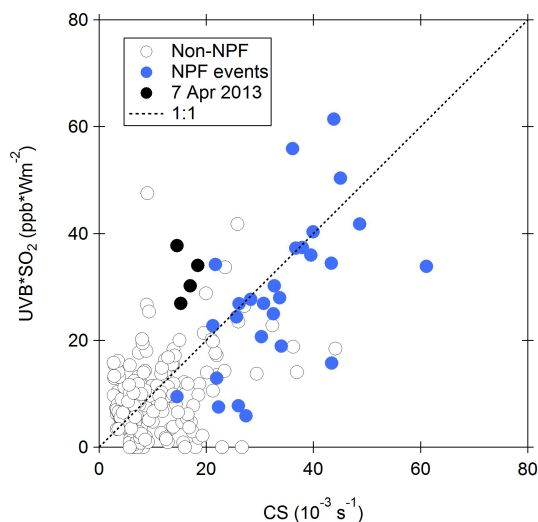


**Figure 7.** Scatter plot of hourly average  $\text{UVB} \cdot \text{SO}_2$  versus condensation sink at noontime (10:00–14:00 LT).

influence of vehicle emission on particle number concentration. The seasonal effects on the emission ratio of PNCs and  $\text{NO}_x$  are rather difficult to address due to the complexity of different controlling factors, such as formation mechanisms and meteorological conditions. For example, Nam et al. (2010) reported a negative exponential correlation between the  $\text{PM}/\text{NO}_x$  ratio in vehicle emission and ambient temperature, and suggested that the impact of ambient temperature on particulate matter was larger than that on  $\text{NO}_x$ . Nevertheless, the observed differences in the PNCs/ $\text{NO}_x$  ratios for winter and summer periods of this study necessitate further investigations on the formation mechanisms of aerosol particles in urban areas, in particular the nucleation and the Aitken modes.

### 3.6 Influence of long-range transport

During the seasons of winter monsoons, i.e., from autumn to spring, continental outflows have been frequently observed in Taipei, which is indicated by the stable northeasterly wind and increase of  $\text{O}_3$  level (Lin et al., 2004). Previous studies of long-range transport of air pollutants on air quality of northern Taiwan showed that an elevated  $\text{PM}_{10}$  was

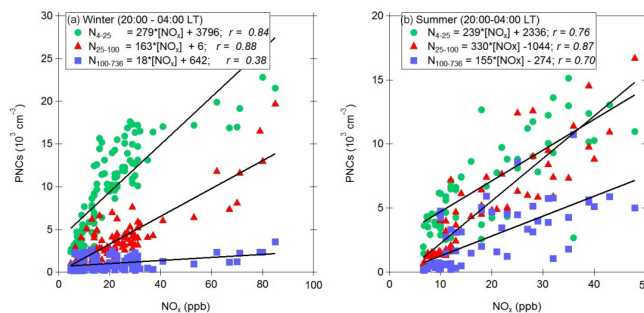


**Figure 8.** Scatter plots for hourly average PNCs vs.  $\text{NO}_x$  measured during the time period of 20:00–04:00 (LT) in (a) winter and (b) summer, with classification of various particle size ranges.

observed under the influence of continental outflows (Lin et al., 2004; Chou et al., 2004). Figure 9 depicts a long-range transport (LRT) pollution event observed at TARO during this study. The wind direction changed from westerly/northwesterly to northeasterly at 21:00, 24 March which continued until 06:00, 26 March. During this period, the  $\text{O}_3$  mixing ratio remained at a moderate level ( $\sim 30$ – $55$  ppb) and  $\text{PM}_{10}$  increased from  $10.0$  to  $98.0 \mu\text{g m}^{-3}$ . It should be noted that the variations of measured pollutants were not solely influenced by long-range transport, but also partly by the variation of local pollution and boundary dynamics. In this section, we attempt to analyze the PSD/PNC under the influences of continental pollution outbreaks. The periods of the respective LRT events are listed in Table S3.

As shown in Fig. 9, the diurnal variations of PSD during the LRT event exhibited two  $N_{4-25}$  peaks associated with the morning and afternoon traffic rush hours; whereas the PNCs of the Aitken-mode particles remained at a low level. The results suggested that the influences of local vehicle emission on PNCs were still in place; whereas growth of particles due to secondary production of condensable vapors could have been suppressed, as NPF was rarely observed during the LRT events. It is noteworthy that a weak dust transport event was observed on 7 April 2013 where a nucleation event was observed in the PSD, evidencing that secondary formation of particles could have had occurred. However, the dominating diameter of particles was  $\sim 40$ – $50$  nm at the initial stage of the event. The nucleation event lasted from  $\sim 06:00$  until 21:00 LT, when the northeasterly wind prevailed. The  $\text{PM}_{10}$  and  $\text{O}_3$  increased from minima of  $44 \mu\text{g m}^{-3}$  (at 06:00 LT) and 25 ppb (at 05:00 LT) to the daily maxima of  $92 \mu\text{g m}^{-3}$  (at 17:00 LT) and 61 ppb (at 16:00 LT). This result showed that the NPF process could have occurred in the upwind area where newly formed particles were transported to the study site, or heterogeneously formed particles were released from the dust surface during the long-range transport of air pollutants (Nie et al., 2014).

The average PSDs for LRT and non-LRT cases are shown in Fig. 10. The GMDs of the nucleation, Aitken, and accumu-

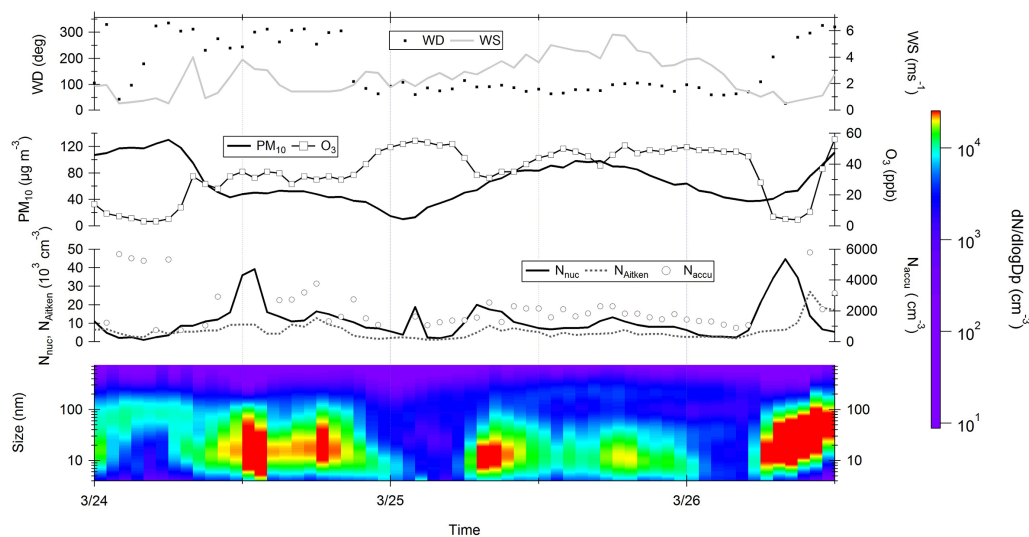


**Figure 9.** Time series of PSD, the  $N_{4-25}$ ,  $N_{25-100}$ ,  $N_{100-736}$ ,  $PM_{10}$ , ozone ( $O_3$ ) and wind direction/speed measured from 24 to 26 March 2013 (from bottom to top).

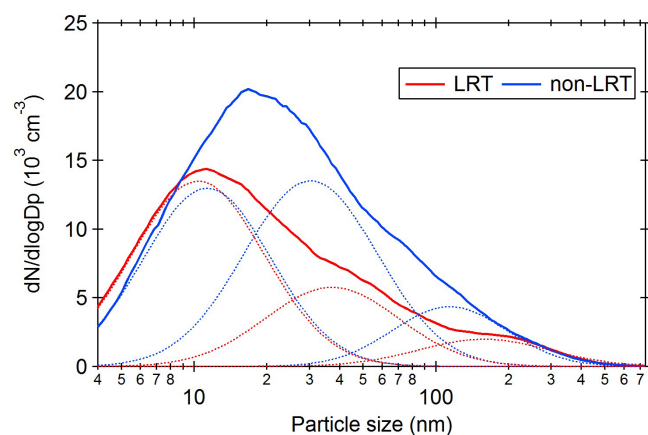


**Figure 10.** Averaged PSDs for LRT and non-LRT episodes measured during the seasons of winter monsoons. Dashed lines illustrate the PSD of each individual mode.

lation modes in PSD were found to be 10.4, 37.2 and 158 nm for LRT and 11.4, 30.4 and 114 nm for non-LRT cases, respectively (see Table S1 for detailed fit results of the PSD for LRT and non-LRT cases). The PNCs of different modes observed in non-LRT events were  $8.6 \times 10^3 \text{ cm}^{-3}$  (nucleation mode),  $9.3 \times 10^3 \text{ cm}^{-3}$  (Aitken mode) and  $2.6 \times 10^3 \text{ cm}^{-3}$  (accumulation mode). The PNCs of LRT events were  $9.2 \times 10^3 \text{ cm}^{-3}$  (nucleation mode),  $4.0 \times 10^3 \text{ cm}^{-3}$  (Aitken mode) and  $1.3 \times 10^3 \text{ cm}^{-3}$  (accumulation mode), respectively. The nucleation-mode PNC observed in non-LRT was comparable with that in LRT events, whereas significantly higher PNCs for the Aitken mode and accumulation mode were observed during non-LRT periods. This was attributed to the lower average wind speed (and hence poor dispersion) during

non-LRT events ( $1.5 \pm 0.8 \text{ m s}^{-1}$ ) than that for LRT events ( $3.0 \pm 0.8 \text{ m s}^{-1}$ ). In contrast to the increase in  $PM_{10}$  usually observed during LRT episodes (e.g., Lin et al., 2012), the relatively lower PNCs suggested that the number concentration of submicron particles, in particular UFPs, was dominated by local emissions. This agreed with the observation of seasonal mass concentration of UFPs that peaked in summertime when Taiwan was isolated from the influences of continental air mass.

#### 4 Conclusions

The mass concentration and chemical composition of ultra-fine particles (UFPs) and submicron particles (i.e.,  $PM_{10}$ ) as well as the particle number concentration (PNC) and size distributions (PSD) with size ranging from 4 to 736 nm were measured during four seasonal campaigns in the period from October 2012 to August 2013 at TARO, a subtropical urban aerosol station in Taipei, Taiwan. Distinct seasonal variability and chemical composition of UFPs and  $PM_{10}$  were revealed. The UFPs were mostly composed of organic matter and reached maxima in summer, whereas the  $PM_{10}$  composition was dominated by ammonium and sulfate, and exhibited a seasonal peak in spring.

It was found that the total PNC was significantly elevated during cold seasons, which was mostly caused by the high level of nucleation-mode particles ( $N_{4-25}$ ). Conversely, both the Aitken-mode ( $N_{25-100}$ ) and accumulation-mode ( $N_{100-736}$ ) PNCs reached their respective maxima in summertime. Consistent correlation without significant seasonal variations was found between the UFPs (i.e., nucleation- and Aitken-mode particles) and  $NO_x$ , suggesting that local vehicle emission was the major source of UFPs in the study area

throughout a year. Local vehicle emission also dominated the accumulation-mode PNC in summer, but not in wintertime. The declined correlation between  $\text{NO}_x$  and  $N_{100-736}$  in winter was likely due to the influences of air pollution associated with the Asian outflows.

The elevated level of UFPs in summer was attributed to the increase in the concentration of Aitken-mode particles ( $N_{25-100}$ ). It was revealed from the measurements of PSD that a large number of nucleation-mode particles could have evolved into the Aitken mode during summertime, which was most likely relevant to the photochemical production of condensable vapors that, in turn, could have contributed to the growth of particles in the atmosphere. Moreover, the chemical measurements suggested that the constituents of the condensed materials in UFPs were mostly organic matter, implying the significance of secondary organic aerosols in the ambient UFPs.

A total of 10 new particle formation (NPF) events occurred out of 84 measurement days in this study, which were observed in autumn (1 out of 23 days), spring (3 out of 26 days) and summer (6 out of 14 days) seasons. The prevalence of NPF in summer agreed with the highest  $\text{H}_2\text{SO}_4$  proxy and lowest  $\text{PM}_{10}$  observed in this study, which provided favorable atmospheric conditions for new particle formation. The average particle growth and formation rates for the NPF events were  $4.0 \pm 1.1 \text{ nm h}^{-1}$  and  $1.4 \pm 0.8 \text{ cm}^{-3} \text{ s}^{-1}$ , respectively, which were comparable to those measured in previous urban studies.

As exemplified above, the characteristics of various physicochemical properties of particles investigated in this study, and the occurrence of NPF, exhibited a strong seasonal variability, which was co-influenced by long-range transported particles during the seasons of winter monsoons and the strong photochemical activities in summer. The results of this study are critical for the authorities involved in urban development and health impact assessment, and the environmental policy makers who are tackling the severe atmospheric pollution in the east Asia region.

**The Supplement related to this article is available online at doi:10.5194/acp-16-1317-2016-supplement.**

*Acknowledgements.* This research was supported by the Academia Sinica and the Ministry of Science and Technology of Taiwan through grants 103-2111-M-001-003, 102-2628-M-001-007 and 101-2119-M-001-003. The authors thank the Taiwan Environmental Protection Administration for providing the air quality and meteorological data. We also thank the Department of Atmospheric Science of National Taiwan University for logistical support of the operation of TARO. Tareq Hussein is gratefully acknowledged for providing us with the code of DO-FIT.

Edited by: T. Petäjä

## References

- Buzorius, G., McNaughton, C. S., Clarke, A. D., Covert, D. S., Blomquist, B., Nielsen, K., and Brechtel, F. J.: Secondary aerosol formation in continental outflow conditions during ACE-Asia, *J. Geophys. Res.*, 109, D24203, doi:10.1029/2004JD004749, 2004.
- Charlson, R. J., Schwartz, S. E., Hales, J. M., Cess, R. D., Coakley Jr., J. A., Hansen, J. E., and Hofmann, D. J.: Climate forcing by anthropogenic aerosols, *Science*, 255, 423–430, 1992.
- Chen, S.-C., Hsu, S.-C., Tsai, C.-J., Chou, Charles, C.-K., Lin, N.-H., Lee, C.-T., Roam, G.-D., and Pui, D. Y. H.: Dynamic variations of ultrafine, fine and coarse particles at the Lu-Lin background site in East Asia, *Atmos. Environ.*, 78, 154–162, 2013.
- Cheng, Y.-H., Kao, Y.-Y., and Liu, J.-J.: Correlations between black carbon mass and size-resolved particle number concentrations in the Taipei urban area: A five-year long-term observation, *Atmos. Pollut. Res.*, 5, 62–72, 2014.
- Cheung, H. C., Wang, T., Baumann, K., and Guo, H.: Influence of regional pollution outflow on the concentrations of fine particulate matter and visibility in the coastal area of southern China, *Atmos. Environ.*, 39, 6463–6474, 2005.
- Cheung, H. C., Morawska, L., and Ristovski, Z. D.: Observation of new particle formation in subtropical urban environment, *Atmos. Chem. Phys.*, 11, 3823–3833, doi:10.5194/acp-11-3823-2011, 2011.
- Cheung, H. C., Chou, C. C.-K., Huang, W.-R., and Tsai, C.-Y.: Characterization of ultrafine particle number concentration and new particle formation in an urban environment of Taipei, Taiwan, *Atmos. Chem. Phys.*, 13, 8935–8946, doi:10.5194/acp-13-8935-2013, 2013.
- Chou, C. C.-K., Lin, C.-Y., Chen, T.-K., Hsu, S.-C., Lung, S.-C., Liu, S. C., and Young, C.-Y.: Influence of Long-Range Transport Dust Particles on Local Air Quality: A Case Study on Asian Dust Episodes in Taipei during the Spring of 2002 Terrestrial, *Atmos. Ocean. Sci.*, 15, 881–889, 2004.
- Chou, C. C.-K., Lee, C.-T., Yuan, C. S., Hsu, W. C., Hsu, S. C., and Liu, S. C.: Implications of the chemical transformation of Asian outflow aerosols for the long-range transport of inorganic nitrogen species, *Atmos. Environ.*, 42, 7508–7519, 2008.
- Chou, C. C.-K., Lee, C. T., Cheng, M. T., Yuan, C. S., Chen, S. J., Wu, Y. L., Hsu, W. C., Lung, S. C., Hsu, S. C., Lin, C. Y., and Liu, S. C.: Seasonal variation and spatial distribution of carbonaceous aerosols in Taiwan, *Atmos. Chem. Phys.*, 10, 9563–9578, doi:10.5194/acp-10-9563-2010, 2010.
- Chow, J. C., Watson, J. G., Chen, L.-W. A., Chang, L. C. O., Robinson, N. F., Trimble, D., and Kohl, S.: The IMPROVE\_A Temperature Protocol for Thermal/Optical Carbon Analysis: Maintaining Consistency with a Long-Term Database, *J. Air Waste Manage. As.*, 57, 1014–1023, 2007.
- Dal Maso, M., Kulmala, M., Riipinen, I., Wagner, R., Hussein, T., Aalto, P. P., and Lehtinen, K. E. J.: Formation and growth of fresh atmospheric aerosols: eight years of aerosol size distribution data from SMEAR II, Hyytiälä, Finland, *Boreal Environ. Res.*, 10, 323–336, 2005.
- Donaldson, K., Li, X. Y., and MacNee, W.: Ultrafine (nanometre) particle mediated lung injury, *J. Aerosol Sci.*, 29, 553–560, 1998.
- Draxler, R. R.: HYSPLIT4 user's guide, NOAA Tech. Memo. ERL ARL-230, NOAA Air Resources Laboratory, Silver Spring, MD, 1999.

- Gao, J., Wang, T., Zhou, X., Wu, W., and Wang, W.: Measurement of aerosol number size distributions in the Yangtze River delta in China: Formation and growth of particles under polluted conditions, *Atmos. Environ.*, 43, 829–836, 2009.
- Harris, S. J. and Maricq, M. M.: Signature size distributions for diesel and gasoline engine exhaust particulate matter, *J. Aerosol Sci.*, 32, 749–764, 2001.
- Holman, J. P.: *Heat Transfer*, New York, McGraw-Hill, 1972.
- Holmes, N. S.: A review of particle formation events and growth in the atmosphere in the various environments and discussion of mechanistic implications, *Atmos. Environ.*, 41, 2183–2201, 2007.
- Hsu, S.-C., Lee, C. S. L., Huh, C.-A., Shaheen, R., Lin, F.-J., and Liu, S. C.: Ammonium Deficiency Caused by Heterogeneous Reactions during a Super Asian Dust Episode, *J. Geophys. Res.*, 119, 6803–6817, doi:10.1002/2013JD021096, 2014.
- Hughes, L. S., Cass, G. R., Gone, J., Ames, M., and Olmez, I.: Physical and Chemical Characterization of Atmospheric Ultrafine Particles in the Los Angeles Area, *Environ. Sci. Technol.*, 32, 1153–1161, 1998.
- Hussein, T., Dal Maso, M., Petäjä, T., Koponen, I. K., Paatero, P., Aalto, P. P., Hämeri, K., and Kulmala, M.: Evaluation of an automatic algorithm for fitting the particle number size distributions, *Boreal Environ. Res.*, 10, 337–355, 2005.
- Kulmala, M.: How Particles Nucleate and Grow, *Science*, 302, 1000–1001, 2003.
- Kulmala, M., Vehkamäki, H., Petäjä, T., Dal Maso, M., Lauri, A., Kerminen, V.-M., Birmili, W., and McMurry, P. H.: Formation and growth rates of ultrafine atmospheric particles: a review of observations, *J. Aerosol Sci.*, 35, 143–176, 2004.
- Kulmala, M., Petäjä, T., Nieminen, T., Sipilä, M., Manninen, H. E., Lehtipalo, K., Dal Maso, M., Aalto, P. P., Junninen, H., Paasonen, P., Riipinen, I., Lehtinen, K. E., Laaksonen, A., and Kerminen, V.-M.: Measurement of the nucleation of atmospheric aerosol particles, *Nature Protocols*, 7, 1651–1667, 2012.
- Lehtinen, K. E. J., Dal Maso, M., Kulmala, M., and Kerminen, V.-M.: Estimating nucleation rates from apparent particle formation rates and vice versa: Revised formulation of the Kerminen-Kulmala equation, *J. Aerosol Sci.*, 38, 988–994, doi:10.1016/j.jaerosci.2007.06.009, 2007.
- Lin, C.-Y., Liu, S. C., Chou, C. C.-K., Liu, T. H., and Lee, C.-T.: Long-Range Transport of Asian Dust and Air Pollutants to Taiwan, *Terr. Atmos. Ocean. Sci.*, 15, 759–784, 2004.
- Lin, C.-Y., Chou, C. C.-K., Wang, Z., Lung, S.-C., Lee, C.-T., Yuan, C.-S., Chen, W.-N., Chang, S.-Y., Hsu, S.-C., Chen, W.-C., and Liu, S. C.: Impact of different transport mechanisms of Asian dust and anthropogenic pollutants to Taiwan, *Atmos. Environ.*, 60, 403–418, 2012.
- Lundgren, D. A., Hlaing, D. N., Rich, T. A., and Marple, V. A.:  $PM_{10}/PM_{2.5}/PM_1$  Data from a Trichotomous Sampler, *Aerosol Sci. Technol.*, 25, 353–357, 1996.
- Marple, V. A., Rubow, K. L., and Behm, S. M.: A Microorifice Uniform Deposit Impactor (MOUDI): Description, Calibration, and Use, *Aerosol Sci. Technol.*, 14, 434–446, 1991.
- Matsumoto, K., Uyama, Y., Hayano, T., Tanimoto, H., Uno, Itsushi, and Uematsu, M.: Chemical properties and outflow patterns of anthropogenic and dust particles on Rishiri Island during the Asian Pacific Regional Aerosol Characterization Experiment (ACE-Asia), *J. Geophys. Res.*, 108, 8666, doi:10.1029/2003JD003426, 2003.
- Morawska, L., Ristovski, Z., Jayaratne, E. R., Keogh, D. U., and Ling, X.: Ambient nano and ultrafine particles from motor vehicle emissions: Characteristics, ambient processing and implications on human exposure, *Atmos. Environ.*, 42, 8113–8138, 2008.
- Nam, E., Kishan, S., Baldauf, R. W., Fulper, C. R., Sabisch, M., and Warila, J.: Temperature Effects on Particulate Matter Emissions from Light-Duty, Gasoline-Powered Motor Vehicles, *Environ. Sci. Technol.*, 44, 4672–4677, 2010.
- Nie, W., Ding, A., Wang, T., Kerminen, V.-M., George, C., Xue, L., Wang, W., Zhang, Q., Petäjä, T., Qi, X., Gao, Xiaomei, Wang, X., Yang, X., Fu, C., and Kulmala, K.: Polluted dust promotes new particle formation and growth, *Scientific Reports*, 4, 6634, 2014.
- Pakkanen, T. A., Kerminen, V.-M., Korhonen, C. H., Hillamo, R. E., Aarnio, P., Koskentalo, T., and Maenhaut, W.: Urban and rural ultrafine ( $PM_{0.1}$ ) particles in the Helsinki area, *Atmos. Environ.*, 35, 4593–4607, 2001.
- Pérez, N., Pey, J., Cusack, M., Reche, C., Querol, X., Alastuey, A., and Viana, M.: Variability of Particle Number, Black Carbon, and  $PM_{10}$ ,  $PM_{2.5}$  and  $PM_1$  Levels and Speciation: Influence of Road Traffic Emissions on Urban Air Quality, *Aerosol Sci. Technol.*, 44, 487–499, 2010.
- Petäjä, T., Mauldin III, R. L., Kosciuch, E., McGrath, J., Nieminen, T., Paasonen, P., Boy, M., Adamov, A., Kotiaho, T., and Kulmala, M.: Sulfuric acid and OH concentrations in a boreal forest site, *Atmos. Chem. Phys.*, 9, 7435–7448, doi:10.5194/acp-9-7435-2009, 2009.
- Pey, J., Rodríguez, S., Querol, X., Alastuey, A., Moreno, T., Putaud, J. P., and Van Dingenen, R.: Variations of urban aerosols in the western Mediterranean, *Atmos. Environ.*, 42, 9052–9062, 2008.
- Pey, J., Querol, X., Alastuey, A., Rodríguez, S., Putaud, J. P., and Van Dingenen, R.: Source apportionment of urban fine and ultrafine particle number concentration in a Western Mediterranean city, *Atmos. Environ.*, 43, 4407–4415, 2009.
- Reche, C., Querol, X., Alastuey, A., Viana, M., Pey, J., Moreno, T., Rodríguez, S., González, Y., Fernández-Camacho, R., de la Rosa, J., Dall'Osto, M., Prévôt, A. S. H., Hueglin, C., Harrison, R. M., and Quincey, P.: New considerations for  $PM$ , Black Carbon and particle number concentration for air quality monitoring across different European cities, *Atmos. Chem. Phys.*, 11, 6207–6227, doi:10.5194/acp-11-6207-2011, 2011.
- Ristovski, Z. D., Jayaratne, E. R., Lim, M., Ayoko, G. A., and Morawska, L.: Influence of diesel fuel sulphur on the nanoparticle emissions from city buses, *Environ. Sci. Technol.*, 40, 1314–1320, 2006.
- Salvador, C. M. and Chou, C. C.-K.: Analysis of semi-volatile materials (SVM) in fine particulate matter, *Atmos. Environ.*, 95, 288–295, 2014.
- Subramanian, R., Khlystov, A. Y., Cabada, J. C., and Robinson, A. L.: Positive and negative artifacts in particulate organic carbon measurements with denuded and undenuded sampler configurations, *Aerosol Sci. Technol.*, 38, 27–48, 2004.
- Turpin, B. J. and Lim, H.-J.: Species contributions to  $PM_{2.5}$  mass concentrations: revisiting common assumptions for estimating organic mass, *Aerosol Sci. Technol.*, 35, 602–610, 2001.

- Vallius, M. J., Ruuskanen, J., Mirme, A., and Pekkanen, J.: Concentrations and Estimated Soot Content of  $PM_{10}$ ,  $PM_{2.5}$  and  $PM_{10}$  in a Subarctic Urban Atmosphere, *Environ. Sci. Technol.*, 34, 1919–1925, 2000.
- Wang, D., Guo, H., Cheung, K., and Gan, F.: Observation of nucleation mode particle burst and new particle formation events at an urban site in Hong Kong, *Atmos. Environ.*, 99, 196–205, 2014.
- Wang, T., Ding, A. J., Blake, D. R., Zahorowski, W., Poon, C. N., and Li, Y.-S.: Chemical characterization of the boundary layer outflow of air pollution to Hong Kong during February–April 2001, 2003.
- Wang, Z. B., Hu, M., Sun, J. Y., Wu, Z. J., Yue, D. L., Shen, X. J., Zhang, Y. M., Pei, X. Y., Cheng, Y. F., and Wiedensohler, A.: Characteristics of regional new particle formation in urban and regional background environments in the North China Plain, *Atmos. Chem. Phys.*, 13, 12495–12506, doi:10.5194/acp-13-12495-2013, 2013.
- Woo, K. S., Chen, D. R., Pui, D. Y. H., and McMurry, P. H.: Measurement of Atlanta aerosol size distribution: observation of ultrafine particle events, *Aerosol Sci. Technol.*, 34, 75–87, 2001.
- Wu, Z., Hu, M., Lin, P., Liu, S., Wehner, B., and Wiedensohler, A.: Particle number size distribution in the urban atmosphere of Beijing, China, *Atmos. Environ.*, 42, 7967–7980, 2008.